JOURNAL OF EXPERIMENTAL AND THEORETICAL PHYSICS, 2024, Vol. 166, No. 1(7), pp. 58–68

SPIN HALL EFFECT MEDIATED CONDUCTION ELECTRON SPIN RESONANCE IN METALS

© 2024 V. V. Ustinov [a,b,*], I. A. Yasyulevich [a,**]

[a] *Mikheev Institute of Metal Physics, Ural Branch of the Russian Academy of Sciences*
[b] *Institute of Natural Sciences and Mathematics, Ural Federal University named after the first President of Russia B. N. Yeltsin*

**e-mail: ustinov@imp.uran.ru*
***e-mail: yasyulevich@imp.uran.ru*

Received February 29, 2024
Revised February 29, 2024
Accepted March 25, 2024

Abstract. The influence of spin-orbit interaction (SOI) on the distribution of spin and charge currents induced in a nonmagnetic conductor by an incident electromagnetic wave is investigated. The effect of SOI on conduction electron spin resonance (CESR) in metals is described. It is established that SOI can significantly alter the CESR line shape. It is shown that this circumstance can be used to determine the SOI magnitude in metal through precision measurements of CESR line asymmetry. The existence of CESR enhancement effect in metals with strong SOI is predicted. It is shown that SOI can lead to enhancement of selective spin transparency and that in a nonmagnetic metal, SOI-induced inversion of electromagnetic wave energy flow can occur – an effect consisting in the emergence of electromagnetic field energy flow directed towards the metal surface in the metal bulk.

Article for a special issue of JETP dedicated to the 130th anniversary of P. L. Kapitsa

DOI: 10.31857/S004445102407e071

1. INTRODUCTION

An electromagnetic wave incident on a conductor induces a high-frequency electric current in it, which prevents its penetration deep into the conductor. The effect of electromagnetic wave amplitude reduction as they penetrate deep into the conductor is called the skin effect [1–3].

An important feature of non-magnetic metals with strong spin-orbit interaction (SOI) is the emergence of coupling between spin and charge currents in such metals [4–12]. Spin-orbit interaction leads to the fact that the flow of electric current in a non-magnetic metal causes the appearance of a transverse pure spin current, which is not accompanied by the transfer of electric charge. This effect is called the spin Hall effect. In the inverse spin Hall effect, the flow of pure spin current in a non-magnetic metal leads to the emergence of a transverse electric charge current.

It can be expected that in metals with strong spin-orbit interaction, high-frequency electric currents induced by electromagnetic waves falling on the metal will generate alternating spin currents (the ac spin Hall effect), which will generate additional high-frequency electric currents (the ac inverse spin Hall effect). The emergence of additional high-frequency electric currents in the conductor due to the presence of spin-orbit interaction will lead to changes in the surface impedance of the metal – a quantity reflecting the relationship between electric current in the conductor and the magnitude of the electric field on its surface.

As is known, the surface impedance determines the power of radio-frequency energy absorbed by the metal per unit time per unit surface area. The derivative of the absorption power of the incident electromagnetic wave with respect to the magnetic field can be found through experiments studying the conduction electron spin resonance.

The conduction electron spin resonance (CESR) in metals with negligible spin-orbit interaction has been studied both theoretically [13–23] and experimentally [24–36]. In works [37–44], it was shown that the increase in the magnitude of spin-orbit interaction between electrons and impurities leads to a decrease in the spin-lattice relaxation time, as some collisions with impurities change the electron spin direction. Consequently, the decrease in spin-lattice relaxation time leads to CESR line broadening. In work [45], a simplified theoretical analysis of the spin-orbit interaction effect on high-frequency electric current distribution in a conducting plate was performed. To simplify calculations, the authors assumed that conduction electrons in metal are affected only by alternating electric field, neglecting the effect of alternating magnetic field. Using this model, the authors found that spin-orbit interaction can influence the surface impedance of the sample.

The purpose of this work is to develop a theory that allows consistently describing the influence of spin-orbit interaction on the distribution of high-frequency electric and spin currents induced in metal by incident electromagnetic wave, and based on it, to provide a description of the spin-orbit interaction effect on conduction electron spin resonance in metals.

2. BASIC EQUATIONS

The equations describing electronic spin transport in conductive materials, taking into account the SOI of conduction electrons with scatterers, are formulated within the microscopic approach in works [46–48]. Here we present these equations for the case when conduction electrons in non-magnetic conductors are affected by electric **E** and magnetic **B** fields, the magnitude and direction of which depend on coordinate **r** and time *t*. Without significant loss of generality, we will consider the conduction electron gas in metal to be degenerate. In these approximations, the equations [46–48] for the density of conduction electrons *N*, vector of electron spin moment density **S**, vector of electron flux density **I** and spin current density tensor $\boldsymbol{J}$ take the form

$$\frac{\partial}{\partial t}N + \frac{\partial}{\partial \mathbf{r}}\cdot\mathbf{I} = 0, \qquad (1)$$

$$\frac{\partial}{\partial t}\mathbf{S} + \frac{\partial}{\partial \mathrm{r}}\cdot\mathbf{J} + \gamma\left[\mathbf{S}\times\mathbf{B}\right] + \frac{1}{\tau_S}\delta\mathbf{S} = 0, \qquad (2)$$

$$\frac{\partial}{\partial t}\mathbf{I} + \frac{v_F^2}{3}\frac{\partial}{\partial \mathrm{r}}\delta N - \frac{e}{m_e}\mathbf{E}N + \frac{e}{m_e c}\left[\mathbf{B}\times\mathbf{I}\right] + \frac{\hbar\gamma}{2m_e}\left(\frac{\partial}{\partial \mathrm{r}}\otimes\mathbf{B}\right)\cdot\mathbf{S} + \frac{1}{\tau_O}\mathbf{I} + \frac{1}{\tau_{SO}}\boldsymbol{\epsilon}\cdot\cdot\boldsymbol{J} = 0, \qquad (3)$$

$$\frac{\partial}{\partial t}\boldsymbol{J} + \frac{v_F^2}{3}\frac{\partial}{\partial \mathrm{r}}\otimes\delta\mathbf{S} - \frac{e}{m_e}\mathbf{E}\otimes\mathbf{S} + \frac{e}{m_e c}\left[\mathbf{B}\times\boldsymbol{J}\right] + \gamma\left[\boldsymbol{J}\times\mathbf{B}\right] + \frac{\hbar\gamma}{2m_e}\left(\frac{\partial}{\partial \mathrm{r}}\otimes\mathrm{B}\right)\delta N + \frac{1}{\tau_O}\mathrm{J} + \frac{1}{\tau_{SO}}\boldsymbol{\epsilon}\cdot\mathbf{I} = 0. \qquad (4)$$

The quantity appearing in equations $\delta N = N - N_0$ is the deviation of electron density N from its equilibrium value N_0, which we consider independent of coordinate **r**, $\delta\mathbf{S} = \mathbf{S} - \mathbf{S}_L$ deviation of spin density **S** from its locally equilibrium value $\mathbf{S}_L = -\chi\mathbf{B}/\mu$, where χ is the Pauli magnetic susceptibility of the electron gas, $\mu = g\mu_B/2$ is the electron magnetic moment with Lande factor equal to g, μ_B is the Bohr magneton, $\gamma = 2\mu/\hbar$ is the gyromagnetic ratio; quantities $e = -|e|$, m_e and v_F are charge, mass and Fermi velocity of conduction electrons respectively; τ_O is momentum relaxation time during orbital motion of electrons, τ_S is spin relaxation time, τ_{SO} is a time-dimensional quantity characterizing the skew spin scattering of electrons due to SOI. The symbol $\boldsymbol{\epsilon}$ denotes an absolutely antisymmetric unit tensor of rank 3, signs "$\otimes$", "$\cdot$" and "$\cdot\cdot$" are used to denote mathematical operations of tensor, scalar and double scalar products of vectors and tensors respectively.

The electric **E** and magnetic **B** fields appearing in equations (1)–(4) can be found from Maxwell's equations:

$$\mathrm{rot}\,\mathbf{E} = -\frac{1}{c}\frac{\partial}{\partial t}\mathbf{B}, \qquad (5)$$

$$\mathrm{rot}\,\mathbf{H} = \frac{4\pi e}{c}\mathbf{I} - \frac{1}{c}\frac{\partial}{\partial t}\mathbf{E}, \qquad (6)$$

where magnetic field induction **B** and field strength **H** are related by

$$\mathbf{B} = \mathbf{H} + 4\pi \mathrm{m}, \tag{7}$$

where $\mathbf{m} = -\mu \mathrm{S}$ is the magnetization of conduction electrons.

From equations (5)–(7) the following equation for the field follows **E**:

$$\mathrm{rotrot}\mathbf{E} = -\frac{4\pi}{c^2}\frac{\partial}{\partial t}\left(e\mathbf{I} + c\,\mathrm{rot}\mathbf{m} - \frac{1}{4\pi}\frac{\partial}{\partial t}\mathbf{E}\right). \tag{8}$$

On the right side of equation (8), there is a sum of three terms in parentheses. The second term, $e\mathbf{I}$, is nothing but the electric current density, i.e., the density of electric charge flow carried by conduction electrons. Второе слагаемое, $c\,\mathrm{rot}\mathbf{m}$, can also be interpreted as the density of a certain current, which has received a special name in literature – "magnetization current". Finally, the third term, $-(1/4\pi)\partial\mathbf{E}/\partial t$, represents the so-called "displacement current". The numerical value of the displacement current for our considered range of frequencies of electric field variation in time is negligibly small, and in further consideration, we will omit this small term in equation (8).

Let in the metal occupying half-space $z \leq 0$, there act an electric field

$$\mathbf{E} = \mathbf{E}^{(\omega)}(z)e^{-i\omega t}$$

and magnetic field

$$\mathbf{B} = \mathbf{B}_0 + \mathbf{B}^{(\omega)}(z)e^{-i\omega t},$$

where $\mathbf{B}_0$ is a constant uniform magnetic field, ω is the frequency of variation of the variable components of electric and magnetic fields. Below we will limit ourselves to considering the case when vectors $\mathbf{E}^{(\omega)}$ and $\mathbf{B}^{(\omega)}$ lie in the plane $z = 0$, and $\mathbf{B}_0 \parallel e_z$, where e_z is a unit vector along the axis z. In the considered geometry, the coordinate dependence of quantities $\delta\mathbf{S}$, $\mathbf{I}$ and $\boldsymbol{J}$ reduces to their dependence only on the coordinate z.

We will limit ourselves to considering systems for which their deviation from the state of electroneutrality can be neglected and the deviation δN can be considered negligibly small compared to N_0. For conductors with metallic conductivity, this condition is fulfilled with high accuracy. A significant simplification in describing spin electronic kinetics is possible under conditions when we can neglect temporal dispersion effects when solving equations (3) and (4), assuming $\omega \ll 1/\tau_O$. We will also assume that the electron spin precession frequency in a constant magnetic field $\Omega = \gamma B_0$ and cyclotron frequency $\Omega_C = |e|B_0/m_e c$ are also small compared to the collision frequency $1/\tau_O$. When writing equations (3) and (4), we omitted terms describing the action on the electron spin of forces caused by the inhomogeneity of field **B**. These effects, discussed in detail previously in work [47], do not play, due to their small magnitude, a fundamental role in the present description of SOI effects. As a result, the system of equations (1)–(4) takes the form

$$\frac{\partial}{\partial t}\mathbf{S} + \frac{\partial}{\partial z}\mathbf{e}_z \cdot \boldsymbol{J} + \tilde{a}\left[\delta\mathbf{S} \times \mathbf{B}\right] + \frac{1}{\tau_S}\delta\mathbf{S} = 0, \tag{9}$$

$$\mathbf{I} = \frac{\sigma_0}{e}\mathbf{E} - \xi\boldsymbol{\epsilon} \cdot\cdot \boldsymbol{J}, \tag{10}$$

$$\boldsymbol{J} = \frac{\sigma_0}{eN_0}\mathbf{E} \otimes \mathbf{S} - D_0\mathbf{e}_z \otimes \frac{\partial}{\partial z}\delta\mathbf{S} - \xi\boldsymbol{\epsilon} \cdot \mathbf{I}, \tag{11}$$

where $\sigma_0 = N_0 e^2 \tau_O / m_e$ is the specific conductivity of free electron gas, $D_0 = v_F^2 \tau_O / 3$ is the electron diffusion coefficient, $\xi = \tau_O / \tau_{SO}$ is a parameter characterizing the relative intensity of the skew spin scattering rate of conduction electrons (relative to momentum relaxation rate). In literature devoted to describing the spin Hall effect (SHE), the term "spin Hall angle" is often used to characterize skew spin scattering, which is denoted as Θ_{SHE}. Generally, for real metals $|\Theta_{SHE}| \ll 1$ and then the parameter we introduced ξ and the spin Hall angle Θ_{SHE} can be simply identified as: $\xi \equiv \Theta_{SHE}$.

Equation (11) clearly describes the "direct" spin Hall effect [4–12]: the conduction electron flow **I**, appearing in the last term of the right-hand side of equation (11), which defines the spin current $\boldsymbol{J}$, induces due to SOI an addition to the spin current equal to $-\xi\boldsymbol{\epsilon} \cdot \mathbf{I}$. Accordingly, equation (10) describes the inverse spin Hall effect: the spin current $\boldsymbol{J}$, appearing in the last term of the right-hand side of equation (10) for **I**, in the presence of SOI induces an addition to the electron flow equal to $-\xi\boldsymbol{\epsilon} \cdot\cdot \boldsymbol{J}$.

Equations (10), (11) can be considered as a system of equations for currents **I** and $\boldsymbol{J}$ at given **E** and **S**. The solution to this system, described in the authors' work [48], can be presented as

$$\boldsymbol{J} = \frac{\sigma}{N_0 e}\mathbf{E}\otimes\mathbf{S} - D\mathbf{e}_z\otimes\frac{\partial}{\partial z}\delta\mathbf{S} - \xi\frac{\sigma}{e}\boldsymbol{\epsilon}\cdot\mathbf{E}, \quad (12)$$

$$\mathbf{I} = \frac{\sigma}{e}\mathbf{E} - \xi D\left[\mathrm{e}_z\times\frac{\partial}{\partial z}\delta\mathbf{S}\right] + \xi\frac{\sigma}{N_0 e}[\mathbf{E}\times\mathbf{S}], \quad (13)$$

where $\sigma = \sigma_0/(1+2\xi^2)$ and $D = D_0\,/\,(1+2\xi^2)$ are conductivity and diffusion coefficient renormalized by spin-orbital interaction, respectively. When obtaining (12), we neglected the weak anisotropy of the diffusion coefficient caused by SOI, which is insignificant for the purposes of this work.

In further consideration, we will assume that the condition $\xi\chi|B_0|\,/\,\mu N_0 \ll 1$, is satisfied, and we will linearize all equations with respect to values $\mathbf{E}^{(\omega)}$, $\mathbf{B}^{(\omega)}$ and $\delta\mathbf{S}$, which allows us to write the expression for $\mathbf{I}$ based on (13) as

$$\mathbf{I} \simeq \frac{\sigma}{e}\mathbf{E} - \xi D\left[\mathbf{e}_z\times\frac{\partial}{\partial z}\delta\mathbf{S}\right]. \quad (14)$$

Using (14), the sum of conductivity current and magnetization current $(e\mathbf{I} + c\,\mathrm{rot}\mathbf{m})$ appearing in equation (8) can be presented as

$$\sigma\mathbf{E} + (1 + \xi eD/\mu c)c\,\mathrm{rot}\mathbf{m}.$$

This means that accounting for SOI when writing the equation for field $\mathbf{E}$ reduces to renormalizing the magnetization current density $c\,\mathrm{rot}\mathbf{m}$ by factor $(1+\xi eD/\mu c)$. In other words, accounting for SOI reduces to replacing the electron magnetic moment value μ appearing in equation (8) with the value

$$\tilde{\mu} = \mu(1 + \xi eD/\mu c).$$

Substituting expression (12) for spin current $\boldsymbol{J}$ into equation (2) and representing spin density $\mathbf{S}$ as

$$\mathbf{S} = -\chi\mathbf{B}\,/\,\mu + \delta\mathbf{S},$$

one can verify that accounting for SOI reduces to renormalizing the Pauli susceptibility value χ appearing in equation (2) by factor $(1+\xi\sigma\mu\,/\,\chi ce)$, i.e., to replacing χ with

$$\tilde{\chi} = \chi(1 + \xi\sigma\mu\,/\,\chi ce).$$

Taking into account the explicit form of values D, σ and χ for metal with degenerate electron gas, it is easy to show that the renormalized values $\tilde{\mu}$, $\tilde{\chi}$ an be written as

$$\tilde{\mu} = \mu(1-\tilde{\xi}), \quad \tilde{\chi} = \chi(1-\tilde{\xi}).$$

The renormalization of both values $\tilde{\mu}$ and $\tilde{\chi}$ is determined by the same parameter $\tilde{\xi}$, which can be written as $\tilde{\xi} = \xi\,/\,\Xi$, where the newly introduced parameter Ξ is defined by expression

$$\Xi = \frac{3g}{8}\frac{\hbar}{\tau_O\varepsilon_F}, \quad (15)$$

in which ε_F is the Fermi energy of conduction electrons.

Substituting expressions (12) and (13) into equations (2) and (8), taking into account

$$\delta\mathbf{S} = \delta\mathbf{S}^{(\omega)}(z)\mathbf{e}^{-i\omega t},$$

after linearization with respect to values $\delta\mathbf{S}^{(\omega)}$ and $\mathbf{E}^{(\omega)}$ we obtain the following system of linear equations for them:

$$L_S^2\frac{\partial^2}{\partial z^2}\delta\mathbf{S}^{(\omega)} - (1 - i\omega\tau_S)\delta\mathbf{S}^{(\omega)} - -\Omega\tau_S\left[\delta\mathbf{S}^{(\omega)}\times\mathbf{e}_z\right] - -L_S^2\frac{\tilde{\chi}c}{\mu D}\left[\mathbf{e}_z\times\frac{\partial}{\partial z}\mathbf{E}^{(\omega)}\right] = 0, \quad (16)$$

$$\delta^2\frac{\partial^2}{\partial z^2}\mathbf{E}^{(\omega)} + 2i\mathbf{E}^{(\omega)} - -\frac{2i\tilde{\mu}c}{\sigma}\left[\mathbf{e}_z\times\frac{\partial}{\partial z}\delta\mathbf{S}^{(\omega)}\right] = 0, \quad (17)$$

where $L_S = \sqrt{D\tau_S}$ is the spin-diffusion length in metal accounting for SOI, $\delta = c\,/\,\sqrt{2\pi\omega\sigma}$ is the skin depth under normal skin effect, determined by electrical conductivity σ.

The system of equations (16), (17) must be supplemented with two boundary conditions that determine the behavior of the field $\mathbf{E}^{(\omega)}(z)$ and spin density $\delta\mathbf{S}^{(\omega)}(z)$ at the boundary $z = 0$. We will assume that on the metal surface $z = 0$ the electric field value is set equal to $\mathbf{E}_0^{(\omega)}$. Then the first of the aforementioned boundary conditions can be written as

$$\mathbf{E}^{(\omega)}(z)\Big|_{z=0} = \mathbf{E}_0^{(\omega)}. \quad (18)$$

We will assume that there are no scattering processes of conduction electrons with spin flip on the metal surface. This condition can be written as a condition of zero $z = 0$ spin current $\boldsymbol{J}(z)$, flowing in the direction $\mathbf{e}_z$ at the surface:

$$\mathbf{e}_z \cdot \boldsymbol{J}(z)\Big|_{z=0} = 0.$$

Taking into account (12) and (18), this boundary condition will be written as

$$\frac{\partial}{\partial z}\delta\mathbf{S}^{(\omega)}\Bigg|_{z=0} = \tilde{\xi}\frac{\chi c}{\mu D}\Big[\mathbf{E}_0^{(\omega)} \times \mathbf{e}_z\Big]. \quad (19)$$

To solve the system of equations (16), (17), let's transition to circular components of the electric field

$$E_\pm = E_x^{(\omega)} \pm iE_y^{(\omega)}$$

and non-equilibrium magnetization of conduction electrons

$$\delta m_\pm = -\mu\left(\delta S_x^{(\omega)} \pm i\delta S_y^{(\omega)}\right).$$

Taking into account boundary conditions (18), (19), we obtain

$$\delta m_\pm = \mp\frac{\Phi_{1(\pm)}}{\kappa_{1(\pm)}}\Psi_{1(\pm)}e^{\kappa_{1(\pm)}z} \mp$$

$$\mp\frac{\Phi_{2(\pm)}}{\kappa_{2(\pm)}}\Psi_{2(\pm)}e^{\kappa_{2(\pm)}z}, \quad (20)$$

$$E_\pm = \Psi_{1(\pm)}e^{\kappa_{1(\pm)}z} + \Psi_{2(\pm)}e^{\kappa_{2(\pm)}z}. \quad (21)$$

Here

$$\Psi_{1(\pm)} = -\frac{E_\pm(0)}{\Phi_{1(\pm)} - \Phi_{2(\pm)}}\left(\Phi_{2(\pm)} + i\tilde{\xi}\frac{\chi c}{D}\right),$$

$$\Psi_{2(\pm)} = \frac{E_\pm(0)}{\Phi_{1(\pm)} - \Phi_{2(\pm)}}\left(\Phi_{1(\pm)} + i\tilde{\xi}\frac{\chi c}{D}\right),$$

$$\Phi_{j(\pm)} = \frac{il_{\chi(\pm)}\kappa_{j(\pm)}^2}{\mathcal{L}_{S(\pm)}^2\kappa_{j(\pm)}^2 - 1},$$

where

$$\kappa_{1(\pm)} = (1 + \lambda_\pm)/\mathcal{L}_\delta, \quad \kappa_{2(\pm)} = (1 - \lambda_\pm)/\mathcal{L}_{S(\pm)},$$

$$\lambda_\pm = l_\sigma l_{\chi(\pm)} / 2\left(\mathcal{L}_{S(\pm)}^2 - \mathcal{L}_\delta^2\right),$$

$$l_{\chi(\pm)} = c\mathcal{L}_{S(\pm)}^2\tilde{\chi}/D, \quad l_\sigma = \left(1 - \tilde{\xi}\right)c/\sigma,$$

$$\mathcal{L}_\delta = -\delta\sqrt{i/2}, \quad \mathcal{L}_{S(\pm)} = L_S / \sqrt{1 \mp i\tau_S(\Omega \pm \omega)}.$$

Solutions for $\delta m_\pm$ and $E_\pm$ in the form were obtained by us for the case when the condition $|\lambda_\pm| \ll 1$ is satisfied. It is easy to see that to satisfy this condition, it is sufficient to require the inequality $\Xi \ll 1$, where Ξ is a parameter, introduced by relation (15). The latter inequality imposes an upper limit on the frequency of electron collisions $1/\tau_O$. Numerical estimates of the parameter Ξ, given in section 4, show that the inequality $\Xi \ll 1$ is satisfied with sufficient accuracy for all metals under the conditions of interest to us.

3. CONDUCTION ELECTRON SPIN RESONANCE IN METAL WITH STRONG SPIN-ORBIT INTERACTION

The circular components of the surface impedance $\varsigma_\pm$ are related to the circular components of the electric field $E_\pm$ and circular components of the magnetic field $H_\pm = H_x^{(\omega)} \pm iH_y^{(\omega)}$ by the relation

$$\varsigma_\pm = \mp i\frac{E_\pm(0)}{H_\pm(0)}. \quad (22)$$

Taking into account the explicit form of solutions (20) and (21) for $\delta m_\pm$ and $E_\pm$ we can find the expression for the field $H_\pm(0)$, included in the impedance definition (22). As a result, for the surface impedance $\varsigma_\pm$ of a non-magnetic metal taking into account SOI, we obtain

$$\varsigma_\pm = \varsigma_0 + \Delta\varsigma_\pm, \quad (23)$$

$$\varsigma_0 = (1 - i)\frac{\omega\delta}{2c}, \quad (24)$$

$$\Delta\varsigma_- = -\pi\chi\frac{\omega^2\delta^3}{cD}\frac{1 + i}{\left(1 - i + r\sqrt{1 + i\alpha}\right)^2} \times$$

$$\times[\left(1 - \tilde{\xi}\right)^2 - 2\left(\frac{1}{r\sqrt{1 + i\alpha}} + \frac{i}{1 + i}\tilde{\xi}^2\right) \times \quad (25)$$

$$\times\left(1 - i + r\sqrt{1 + i\alpha}\right)],$$

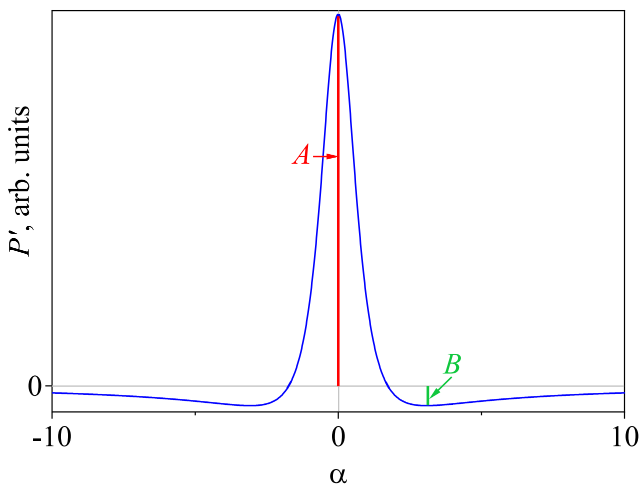

Fig. 1. Derivative of the power absorbed by the sample with respect to magnetic field $P'(\alpha)$ under CESR conditions in metal at $\delta \ll L_S$

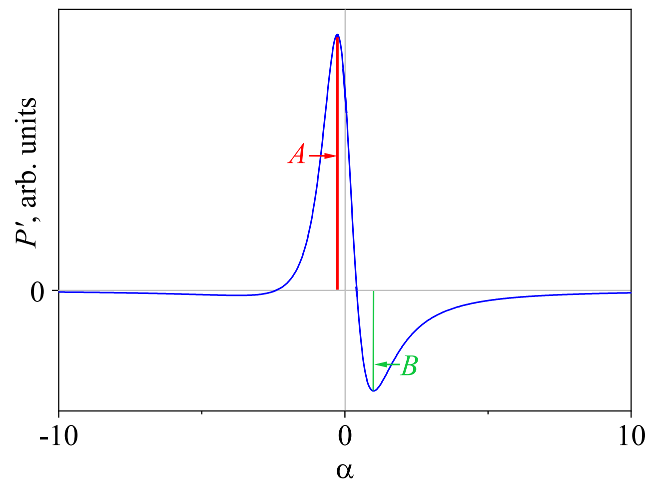

Fig. 2. Derivative of the power absorbed by the sample with respect to magnetic field $P'(\alpha)$ under CESR conditions in metal at $\delta \gg L_S$ and $\xi^2 \ll L_S / \delta$

where $\alpha = (\Omega - \omega)\tau_S$ is the parameter determining the dependence of surface impedance on external magnetic field, $r = \delta / L_S$ is the parameter characterizing the ratio of skin depth δ and spin diffusion length L_S. The expression for $\Delta\varsigma_+$ can be obtained from formula (25) by replacing Ω with $-\Omega$ in the expression for α.

The power of energy absorbed by metal per unit time per unit area of its surface can be found using the formula

$$P = \frac{c}{4\pi}\mathrm{Re}\left[\varsigma_0 + \eta_+\Delta\varsigma_+ + \eta_-\Delta\varsigma_-\right]\left|\mathbf{H}^{(\omega)}(0)\right|^2. \quad (26)$$

Here $\eta_\pm$ are real numbers determined through the polarization vector of the alternating magnetic field at the boundary $\mathbf{h}^{(\omega)}(0) \equiv \mathbf{h}^{(\omega)}$ by relations

$$\eta_\pm = \frac{1}{2}\left(1 \mp i\mathbf{h} \cdot \left[\mathbf{h}^{(\omega)} \times \mathbf{h}^{(\omega)*}\right]\right),$$
$$\mathbf{h}^{(\omega)} \cdot \mathbf{h}^{(\omega)*} = 1,$$

where $\mathbf{h}$ — a unit vector codirectional with the vector of constant uniform magnetic field, the sign "*" denotes complex conjugation operation. For linear field polarization $\mathbf{H}^{(\omega)}$ values $\eta_\pm = 1/2$.

The experimentally observed quantity is usually the derivative of the power absorbed by the sample with respect to magnetic field $P' = dP / dB_0$, which has a singularity as a function of magnetic field near the resonant value B_r, determined from the condition $\gamma B_r = \omega$. Near resonance, the contribution of the smoothly varying function $\Delta\varsigma_+$ to P' is small and the signal P' as a function of magnetic field B_0, expressed in dimensionless variables $\alpha = \gamma\tau_S(B_0 - B_r)$, is proportional to the derivative with respect to α of the real part of impedance $\Delta\varsigma_-$:

$$P'(\alpha) \sim \frac{d}{d\alpha}\mathrm{Re}\Delta\varsigma_-. \quad (27)$$

Let's analyze the influence of SOI on the signal shape $P'(\alpha)$, obtained by substituting expression (25) into (27).

Let the skin depth δ be small compared to the spin diffusion length L_S. Then $r \ll 1$ and in main approximation for the small parameter r we obtain

$$P'(\alpha) \sim \frac{d}{d\alpha}\mathrm{Re}\frac{i}{\sqrt{1 + i\alpha}}. \quad (28)$$

In this case, the spin-orbital interaction practically does not affect the signal shape $P'(\alpha)$. The shape of the CESR signal curve, defined by expression (28), was first described by Dyson [13] and therefore later became known as "Dyson lineshape". Fig. 1 shows the CESR signal line CESR $P'(\alpha)$, constructed using expression (28).

The Dyson lineshape signal of CESR $P'(\alpha)$ in Fig. 1 represents a curve that is symmetric with respect to the ordinate axis $\alpha = 0$ and asymmetric with respect to the abscissa axis

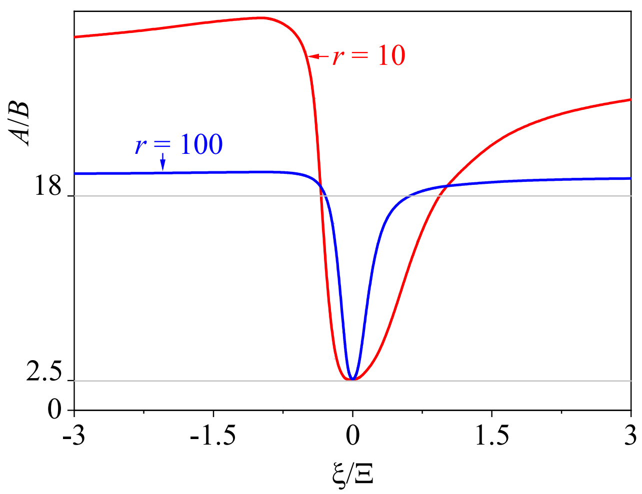

Fig. 3. The influence of spin-orbit interaction on the line asymmetry parameter A / B at $r = 10$ (red curve) and $r = 100$ (blue curve)

$P' = 0$. The aforementioned asymmetry is characterized by A / B, where A — the "height" of the curve maximum $P'(\alpha)$, and B is the "depth" of the minimum lying in the region of magnetic field values greater than resonant $(\alpha > 0)$. The lengths A and B are highlighted in Fig. 1 in red and green colors respectively. For the Dyson lineshape of the CESR signal $P'(\alpha)$ the signal asymmetry indicator $A / B \approx 18$.

Let the skin depth δ be large compared to the spin diffusion length L_S, then the parameter $r \gg 1$.

In the case when $r \gg 1$, and the SOI intensity is extremely low, so that the condition $\tilde{\xi}^2 \ll 1 / r \ll 1$, is met, from formula (25) we obtain that

$$P' \sim \frac{d}{d\alpha}\frac{1+\alpha}{1+\alpha^2}. \tag{29}$$

In this limiting case, the influence of SOI on the CESR line shape is also not significant. The line shape of the CESR signal described by formula (29) is called "Lorentzian lineshape". Fig. 2 shows the Lorentzian lineshape of the CESR signal $P'(\alpha)$, given by expression (29). For the Lorentzian lineshape of the CESR signal $P'(\alpha)$ the value of the resonance line asymmetry indicator $A / B \approx 2.5$.

In the case when $r \gg 1$, and the SOI intensity is sufficiently high, so that the condition $\tilde{\xi}^2 \gg 1 / r$, is met, from formula (25) we obtain

$$P' \sim \tilde{\xi}^2 \frac{d}{d\alpha} \mathrm{Re} \frac{i}{\sqrt{1 + i\alpha}}. \tag{30}$$

In this case, SOI has the most significant influence on the line shape and amplitude of the CESR signal: the CESR signal shape in this case is close to Dyson lineshape and the signal magnitude P' is directly proportional to the square of the spin Hall angle. Thus, if $\delta \gg L_S$, then in conductors with strong spin-orbit interaction, when the condition $\tilde{\xi}^2 \gg L_S / \delta$ is met, the CESR enhancement effect may be observed.

In the case of an arbitrary ratio of parameter values $\tilde{\xi}^2$ and $1 / r$ from (25), it follows that

$$P' \sim \frac{d}{d\alpha}\left(\frac{1 + 2\tilde{\xi} - \tilde{\xi}^2}{2r}\frac{1+\alpha}{1+\alpha^2} + \tilde{\xi}^2 \mathrm{Re}\frac{i}{\sqrt{1+i\alpha}}\right). \tag{31}$$

The CESR signal in this case, according to (31), is the sum of two signals: a Lorentzian lineshape signal (the first term in parentheses in expression (31)) and a Dyson lineshape signal (the second term in parentheses). The relative magnitude of these signals is determined by the ratio of parameters $\tilde{\xi}^2$ and $1 / r$. Obviously, the line asymmetry parameter of the CESR line (31) will significantly change with variations in $\tilde{\xi}$, and the nature of this dependence will be determined by the value of the ratio $r = \delta / L_S$. The results of numerical calculation of the line asymmetry parameter A / B dependence on $\tilde{\xi}$ are shown in Fig. 3.

Fig. 3 clearly demonstrates the fact that measurements of the line asymmetry parameter A / B of the CESR line can provide quantitative information about the magnitude of spin-orbit interaction in the conductor, which determines the value of the spin Hall angle ξ.

Comparing the CESR line shape in two limiting cases: $\delta \gg L_S$ and $\delta \ll L_S$, we note an important pattern. If the spin-orbit interaction is sufficiently strong, so that under the condition $\delta \gg L_S$ the inequality $\xi \gg \Xi\sqrt{L_S / \delta}$, is satisfied, then the theory predicts that in each of the aforementioned limiting cases, the CESR line shape will be close to Dyson lineshape. Therefore, the experimental observation of a CESR signal in metal with a shape close to Dyson lineshape at any ratio of skin depth and spin diffusion length can be qualitatively interpreted as the presence of strong spin-orbit interaction in this metal.

4. INFLUENCE OF SPIN-ORBIT INTERACTION ON SELECTIVE SPIN TRANSPARENCY OF METAL

Selective spin transparency is the phenomenon of electromagnetic field penetration into a conductor to a depth significantly exceeding the skin depth, due to the diffusive transport of non-equilibrium magnetization of conduction electrons deep into the metal [14–16, 49–51]. The phenomenon of selective spin transparency is observed under CESR conditions when the precession frequency of the electron spin Ω in the magnetic field is close to the alternating field frequency ω. Of the two circular components of the electric field we found, E_+ and E_- only the component E_- demonstrates behavior characteristic of the selective spin transparency phenomenon.

For the field component E_- from expression (21) in the case when $\delta \ll L_S$, taking into account the condition $|\lambda_-| \ll 1$ we obtain

$$E_-(z) = E_-(0)\Big\{\Big[1-\big(1-\tilde{\xi}\big)\Xi^2\Big]e^{z/\mathcal{L}_\delta} + \\ +\big(1-\tilde{\xi}\big)\Xi^2 e^{z/\mathcal{L}_{S(-)}}\Big\}. \quad (32)$$

It is evident that under the considered conditions, the electric field E_- can be represented as the sum of two parts: a large rapidly decaying part (at distances of the order of δ),

$$E_-(0)e^{z/\mathcal{L}_\delta},$$

and a small slowly decaying part (at distances of the order of L_S),

$$E_-(0)\Xi^2\big(1-\tilde{\xi}\big)e^{z/\mathcal{L}_{S(-)}}.$$

The small slowly decaying part arises due to the diffusive transport of non-equilibrium spin density of conduction electrons deep into the metal at distances significantly exceeding the skin depth.

From result (32), it follows that SOI significantly affects the magnitude of the small slowly decaying part of the electric field. In conductors with negative spin Hall angle $\xi < 0$ or conductors where $\xi > 2\Xi$, the slowly decaying part will definitely be larger than in conductors where SOI is negligibly small. Thus, metals with negative spin Hall angle and metals where the spin Hall angle exceeds the value 2Ξ may demonstrate the effect of enhanced selective spin transparency.

Let's consider how SOI affects the penetration of electromagnetic field energy flux into the metal under CESR conditions. For this purpose, we will calculate the dependence of the Poynting vector on coordinate z

$$\mathbf{U} = \frac{c}{4\pi}\big[\mathbf{E}\times\mathbf{H}\big].$$

The time-averaged z-component of the Poynting vector $\bar{U}_z$ under resonance conditions (at $\alpha = 0$) in the case when $\delta \ll L_S$, can be written as

$$\bar{U}_z(z) \approx -\bar{U}_z(0)\left[e^{2z/\delta} + \big(1-\tilde{\xi}\big)\Xi^4\frac{2L_S}{\delta}e^{2z/L_S}\right]. \quad (33)$$

From (33) it follows that: 1) the time-averaged electromagnetic field energy flux near the metal surface at distances of the order of skin depth ($|z| \le \delta$) is directed into the metal; 2) at distances significantly exceeding the skin depth but comparable to the spin diffusion length ($\delta \ll |z| \le L_S$), the time-averaged electromagnetic field energy flux can flow in different directions depending on the magnitude of the spin Hall angle ξ. If the spin Hall angle ξ is positive and small compared to the parameter value Ξ or negative, then the time-averaged energy flux at $\delta \ll |z| \le L_S$ is directed into the metal. However, if SOI is sufficiently large so that $\xi > \Xi$, then the aforementioned flux is directed towards the metal surface.

Thus, a sufficiently large SOI can cause the effect of energy flow direction inversion of electromagnetic waves deep in the metal under conditions of selective spin transparency. The physical cause of the energy flow direction inversion effect of electromagnetic waves is the fact that the spin current induced in the metal generates, due to the inverse spin Hall effect, an additional electric current that is opposite to the magnetization current arising under the action of an alternating electromagnetic field. In the case when $\xi > \Xi$, at depths $\delta \ll |z| \le L_S$ the additional electric current arising due to SOI exceeds the magnetization current in magnitude, which causes the electromagnetic field energy flow directed opposite to the electromagnetic field energy flow within the skin layer.

Let us perform numerical estimates of the parameter Ξ and parameter $\tilde{\xi} = \xi / \Xi$ for some non-magnetic metals for which the spin Hall angle values have been experimentally determined. The table contains characteristics of metals Al, Cu, Nb, Ag, Pt and Au, which we will use for numerical estimation of the parameters of interest.

The second column of the table shows data on the charge carrier concentration N_0 in the metal. The third column contains the values of the metal's specific electrical resistivity. The resistivity values for Al, Cu, Nb, Ag and Au are given for temperature 273 K, and for Pt – for temperature 300 K. The fourth column contains data on the spin Hall angle Θ_{SHE} in the metal. Data on the values of N_0 and ρ for Al, Cu, Nb, Ag and Au are taken from [52], for Pt — from [53]. Data on the values of Θ_{SHE} for all metals are taken from review [11].

For order-of-magnitude estimates, we will consider the electron gas to be degenerate, the electron dispersion law to be isotropic and quadratic, set the effective electron mass equal to the free electron mass m_e, and the value of the g-factor. In this simplest model, the Fermi energy of free electron gas

$$\varepsilon_F = \frac{\hbar^2 \left(3\pi^2 N_0\right)^{2/3}}{2m_e}.$$

From the Drude formula for electron gas conductivity, we obtain an estimate for the electron momentum relaxation time $\tau_O = m_e / \rho e^2 N_0$. The table presents values of parameter $\Xi = 3g\hbar / 8\tau_O \varepsilon_F$, calculated using data for N_0 and ρ, shown in the table. To find parameter $\tilde{\xi}$ we use expression $\tilde{\xi} = \Theta_{SHE} / \Xi$.

The table shows that for all considered metals, there is a strong inequality $\Xi \ll 1$, which we used in deriving analytical expressions for fields.

he table also shows that in metals such as Cu, Nb, Ag, Pt and Au, parameter $\tilde{\xi}$ can reach a significant value and, consequently, in these metals, the influence of SOI on the CESR line shape can be detected experimentally.

Estimates shown in the table indicate that in metals such as Nb, Pt and Au, the effect of enhanced selective spin transparency can be detected.

5. CONCLUSION

The developed theory allowed us to describe the influence of spin-orbit interaction on the distribution of high-frequency electric and spin currents induced in a non-magnetic metal by an incident electromagnetic wave. It is shown that: 1) SOI causes the emergence of additional spin density competing with the spin density arising in the metal under the action of an alternating magnetic field; 2) the alternating spin current induced by the wave in the metal under the influence of SOI, due to the inverse spin Hall effect, generates an additional electric current that is opposite to the

Table. Data on characteristics of metals Al, Cu, Nb, Ag, Pt and Au equal to 2.

Metal	N_0, cm^{-3}	ρ, μΩ·cm	Θ_{SHE}	Ξ	$\tilde{\xi}$
Al	$18.1 \cdot 10^{22}$	2.4	$0.0001 \div 0.0003$	$5 \cdot 10^{-3}$	$0.02 \div 0.06$
Cu	$8.5 \cdot 10^{22}$	1.6	0.003	$3 \cdot 10^{-3}$	1
Nb	$5.6 \cdot 10^{22}$	15.2	−0.0087	$22 \cdot 10^{-3}$	−0.39
Ag	$5.9 \cdot 10^{22}$	1.5	0.007	$2 \cdot 10^{-3}$	3.5
Pt	$1.6 \cdot 10^{22}$	16.8	$0.004 \div 0.1$	$16 \cdot 10^{-3}$	$0.25 \div 6.25$
Au	$5.9 \cdot 10^{22}$	2	$0.002 \div 0.11$	$3 \cdot 10^{-3}$	$0.67 \div 36.67$

magnetization current arising under the action of the electromagnetic field.

The surface impedance of metal has been calculated taking into account SOI, and the features of the conduction electron spin resonance line shape caused by SOI action are described. It is shown that spin-orbital interaction under CESR conditions can significantly influence the shape of the derivative of power absorbed by the sample with respect to magnetic field. The influence of SOI on line asymmetry parameter of the derivative of power absorbed by the sample with respect to magnetic field has been studied, demonstrating that precise measurements of the CESR line shape can provide information about the SOI magnitude in the metal under study.

It is shown that SOI can lead to the effect of enhanced selective spin transparency, which consists in the increase of the amplitude of slowly decaying part of the electric field arising from diffusive transfer of non-equilibrium spin density of conduction electrons deep into the metal at distances significantly exceeding the skin depth.

The influence of SOI on the energy flux density of electromagnetic field penetrating into the metal has been studied. It is shown that in a semi-bounded non-magnetic metal, SOI-induced inversion of electromagnetic wave energy flow direction can occur – an effect consisting in the emergence of electromagnetic field energy flow directed towards the metal surface in the metal depth. The nature of this effect lies in the fact that the spin current induced in the metal by electromagnetic wave under SOI influence, under conditions of inverse spin Hall effect, generates additional electric current, whose density vector is directed against the magnetization current density vector, and whose vector magnitude exceeds that of the magnetization current.

FUNDING

The work was carried out within the state assignment of the Ministry of Education and Science of Russia (subject Spin, No. 122021000036-3). I. A. Yasyulevich thanks the M.N. Mikheev Institute of Metal Physics for supporting his work under the state assignment of the Ministry of Education and Science of Russia on the subject Spin, which was carried out within the youth project of IMP UB RAS No. m 2-23.

REFERENCES

1. I. M. Lifshitz, M. I. Kaganov, Sov. Phys. Usp. 8, 805 (1966).

2. E. A. Kaner, V. G. Skobov, Sov. Phys. Usp. 9, 480 (1967).

3. E. A. Kaner, V. F. Gantmakher, Sov. Phys. Usp. 11, 81 (1968).

4. M. I. Dyakonov, V. I. Perel, JETP Letters 13, 467 (1971).

5. M. I. Dyakonov and V. I. Perel, Phys. Lett. A 35, 459 (1971).

6. J.-N. Chazalviel, Phys. Rev. B 11, 3918 (1975).

7. J. E. Hirsch, Phys. Rev. Lett. 83, 1834 (1999).

8. S. Zhang, Phys. Rev. Lett. 85, 393 (2000).

9. A. Hoffmann, IEEE Trans. Magn. 49, 5172 (2013).

10. Y. Niimi and Y. Otani, Rep. Prog. Phys. 78, 124501 (2015).

11. J. Sinova, S. O. Valenzuela, J. Wunderlich, C. H. Back, and T. Jungwirth, Rev. Mod. Phys. 87, 1213 (2015).

12. Spin Physics in Semiconductors, ed. by M. I. Dyakonov, Springer Int. Publ., Cham (2017), p. 532.

13. F. J. Dyson, Phys. Rev. 98, 349 (1955).

14. I. M. Lifshitz, M. Ya. Azbel', and V.I. Gerasimenko, J. Phys. Chem. Solids 1, 164 (1956).

15. M. Ya. Azbel', V. I. Gerasimenko, I. M. Lifshitz, *Sov. Phys*. JETP **5**, 986 (1957).

16. M. Ya. Azbel', V. I. Gerasimenko, I. M. Lifshitz, Sov. Phys. JETP 4, 276 (1957).

17. M. Lampe and P. M. Platzman, Phys. Rev. 150, 340 (1966).

18. M. B. Walker, Can. J. Phys. 48, 111 (1970).

19. M. B. Walker, Phys. Rev. B 3, 30 (1971).

20. B. M. Khabibullin, É. G. Kharakhash'yan, Sov. Phys. Usp. 16, 806 (1974).

21. W. S. Glaunsinger and M. J. Sienko, J. Magn. Reson. 1969 10, 253 (1973).

22. V. V. Ustinov, Phys. Met. Metallogr. 45, 473 (1978).

23. V. V. Ustinov and D. Z. Khusainov, Phys. Status Solidi B 110, 363 (1982).

24. T. W. Griswold, A. F. Kip, and C. Kittel, Phys. Rev. 88, 951 (1952).

25. G. Feher and A. F. Kip, Phys. Rev. 98, 337 (1955).

26. J. Konopka, Phys. Lett. A 26, 29 (1967).

27. J. H. Pifer and R. Magno, Phys. Rev. B 3, 663 (1971).

28. R. Magno and J. H. Pifer, Phys. Rev. B 10, 3727 (1974).

29. P. Damay and M. J. Sienko, Phys. Rev. B 13, 603 (1976).

30. J. E. Wertz and J. R. Bolton, Electron Spin Resonance: Elementary Theory and Practical Applications, Chapman and Hall, New York (1986), p. 500.

31. M. Fanciulli, T. Lei, and T. D. Moustakas, Phys. Rev. B 48, 15144 (1993).

32. A. Janossy, O. Chauvet, S. Pekker, J. R. Cooper, and L. Forro, Phys. Rev. Lett. 71, 1091 (1993).

33. M. Danilczuk, A. Lund, J. Sadlo, H. Yamada, and J. Michalik, Spectrochim. Acta A: Mol. Biomol. Spectrosc. 63, 189 (2006).

34. K. Tadyszak, R. Strzelczyk, E. Coy, M. Mackowiak, and M. A. Augustyniak-Jablokow, Magn. Reson. Chem. 54, 239 (2016).

35. P. G. Baranov, H. J. Von Bardeleben, F. Jelezko, and J. Wrachtrup, Magnetic Resonance of Semiconductors and Their Nanostructures: Basic and Advanced Applications, Springer Vienna, Vienna (2017), p. 524.

36. J. A. Bau, A.-H. Emwas, and M. Rueping, iScience 25, 105360 (2022).

37. R. N. Edmonds, M. R. Harrison, and P. P. Edwards, Annu. Rep. Sect. C Phys. Chem. 82, 265 (1985).

38. J. R. Asik, M. A. Ball, and C. P. Slichter, Phys. Rev. Lett. 16, 740 (1966).

39. J. R. Asik, M. A. Ball, and C. P. Slichter, Phys. Rev. 181, 645 (1969).

40. M. A. Ball, J. R. Asik, and C. P. Slichter, Phys. Rev. 181, 662 (1969).

41. J. H. Pifer, Phys. Rev. B 12, 4391 (1975).

42. V. Zarifis and T. G. Castner, Phys. Rev. B 36, 6198 (1987).

43. V. Zarifis and T. G. Castner, Phys. Rev. B 57, 14600 (1998).

44. R. B. Morgunov, A. I. Dmitriev, F. B. Mushenok, O. L. Kazakova, Semiconductors 43, 896 (2009).

45. P. S. Alekseev and M. I. Dyakonov, Phys. Rev. B 100, 081301 (2019).

46. V. V. Ustinov, I. A. Yasyulevich, Phys. Met. Metallogr. 121, 223 (2020).

47. V. V. Ustinov and I. A. Yasyulevich, Phys. Rev. B 102, 134431 (2020).

48. V. V. Ustinov, I. A. Yasyulevich, and N. G. Bebenin, Phys. Met. Met. 124, 1745 (2023).

49. N. S. VanderVen and R. T. Schumacher, Phys. Rev. Lett. 12, 695 (1964).

50. R. B. Lewis and T. R. Carver, Phys. Rev. 155, 309 (1967).

51. L. I. Medvedev, R. G. Mustafin, I. G. Zamaleev, É. G. Kharakhash'yan, JETP Lett. 38, 274 (1983).

52. N. W. Ashcroft and N. D. Mermin, Solid State Physics, Harcourt College Publishers, New York (1976), p. 826

53. G. Fischer, H. Hoffmann, and J. Vancea, Phys. Rev. B 22, 6065 (1980).